Diversity of Serine Hydrolase Activities of Unchallenged and *Botrytis*-infected *Arabidopsis thaliana*[*]

Farnusch Kaschani‡§, Christian Gu‡§, Sherry Niessen¶, Heather Hoover¶, Benjamin F. Cravatt¶, and Renier A. L. van der Hoorn‡‖[**]

Activity-based protein profiling is a powerful method to display enzyme activities in proteomes and provides crucial information on enzyme activity rather than protein or transcript abundance. We applied activity-based protein profiling using fluorophosphonate-based probes to display the activities of Ser hydrolases in the model plant *Arabidopsis thaliana*. Multidimensional protein identification technology and in-gel analysis of fluorophosphonate-labeled leaf extracts revealed over 50 Ser hydrolases, including dozens of proteases, esterases, and lipases, representing over 10 different enzyme families. Except for some well characterized Ser hydrolases like subtilases TPP2 and ARA12, prolyl oligopeptidase acylamino acid-releasing enzyme, serine carboxypeptidase-like SNG1 and BRS1, carboxylesterase-like CXE12, methylesterases MES2 and MES3, and *S*-formylglutathione hydrolase, the majority of these serine hydrolases have not been described before. We studied transiently expressed SNG1 and investigated plants infected with the fungal pathogen *Botrytis cinerea*. Besides the down-regulation of several *Arabidopsis* Ser hydrolase activities during *Botrytis* infection, we detected the activities of *Botrytis*-derived cutinases and lipases, which are thought to contribute to pathogenicity. *Molecular & Cellular Proteomics 8: 1082–1093, 2009.*

Serine hydrolases comprise a large collection of enzymes from different structural classes that fulfill diverse biochemical roles such as proteases, lipases, esterases, and transferases. The *Arabidopsis* genome encodes for hundreds of serine hydrolases that belong to dozens of large multigene families (1). Common to these enzymes is that the active site contains an activated serine residue that performs the nucleophilic attack on the substrate, resulting in a covalent intermediate.

To study the diverse roles of serine hydrolases in plants and in other organisms in detail, it is essential to display the activities of these enzymes because enzyme activities depend on various post-translational processes like phosphorylation, nitrosylation, processing, cofactors, and inhibitors, and prediction of enzyme activities from transcriptomics or proteomics data can be misleading. Serine hydrolase activities can be displayed through activity-based protein profiling (ABPP).[1] ABPP is based on the use of fluorescent or biotinylated small molecules that irreversibly react with the active site of enzymes in a mechanism-dependent manner and has been pioneered by Cravatt and Bogyo and co-workers (2, 3). Active site accessibility and reactivity is an important indication for enzyme activity (4). Labeled enzymes can be displayed on protein gels and blots or identified by mass spectrometry.

A frequently used probe for serine hydrolases is based on fluorophosphonate (FP), which is also the reactive moiety in the broad range serine hydrolase inhibitor diisopropyl fluorophosphonate. When used on mammalian extracts, FP probes display dozens of serine hydrolase activities, including proteases, lipases, and esterases (5, 6). FP probes do not label zymogen or inhibitor-bound serine hydrolases demonstrating that FP probes label only active enzymes (6). Serine hydrolase profiling with FP has proved extremely useful to detect altered enzyme activities and identify inhibitors. For example, FP profiling has been used to find diagnostic markers for cancer invasiveness (7, 8) and to detect the selectivity of drugs that target *e.g.* fatty acid amide hydrolase (9, 10).

In plants, the roles of Ser hydrolases are even more diverse because many of these enzymes act in the production of elaborate secondary metabolites. Carboxypeptidase-like SNG1, for example, acts as an acyltransferase in the production of sinapoylmalate (11), and some GDSL lipase-like proteins act as sinapine esterases (12). Furthermore carboxylesterase-like CXE12 activates herbicides by hydrolysis (13), and several

From the ‡Plant Chemetics laboratory, Max Planck Institute for Plant Breeding Research, Carl-von-Linné Weg 10, 50829 Cologne, Germany, the ‖Chemical Genomics Centre of the Max Planck Society, Otto Hahn Strasse 15, 44227, Dortmund, Germany, and ¶The Skaggs Institute for Chemical Biology and Department of Chemical Physiology, The Center for Physiological Proteomics, The Scripps Research Institute, La Jolla, California 92037

Received, October 30, 2008, and in revised form, January 8, 2009
Published, MCP Papers in Press, January 11, 2009, DOI 10.1074/mcp.M800494-MCP200

[1] The abbreviations used are: ABPP, activity-based protein profiling; Bio, biotin; CXE, carboxylesterase; FP, fluorophosphonate; MES, methylesterase; MudPIT, multidimensional protein identification technology; PEG, polyethylene glycol; POPL, prolyl oligopeptidase-like protein; Rh, rhodamine; SCPL, serine carboxypeptidase-like protein; dpi, days postinfection; SCX, strong cation exchange; 1D, one-dimensional; Rubisco, ribulose-bisphosphate carboxylase/oxygenase.

methylesterases hydrolyze methylated phytohormones like salicylic acid, jasmonic acid, and indoleacetic acid (14).

To study the role of serine hydrolases in plants further, we applied serine hydrolase profiling using FP-based probes on *Arabidopsis* leaf extracts. So far, serine hydrolase profiling in plants was limited to a single study where four FP-labeled enzymes were identified from *Arabidopsis* leaf extracts. These labeled proteins were prolyl oligopeptidase At1g76140, carboxypeptidase CXE12 (At3g48690), serine hydrolase At5g20060, and a GDSL lipase (13). In this study, we used multidimensional protein identification technology (MudPIT) and in-gel digestions to identify over 50 serine hydrolase activities in *Arabidopsis* leaf extracts. The serine hydrolase activities that were identified are classified and studied in plants during infection with the necrotrophic pathogen *Botrytis cinerea*.

EXPERIMENTAL PROCEDURES

Sample Preparation—The synthesis of the probes has been described previously: FPpBio (15), FPpRh (15), FP-Rh (5), and TriFP (13). Unless otherwise stated all reagents used in this study are of the highest grade available. All solvents were MS or HPLC grade.

Plant leaf extracts were obtained by grinding 2 g of frozen leaves of 4-week-old *Arabidopsis thaliana* ecotype Col-0 in a mortar at room temperature (22–24 °C) to a homogenous green paste. The paste was mixed with 5–6 ml of distilled water or 1× PBS (Invitrogen) and cleared by centrifugation (5 min at 16,000 × *g*). 500-μl aliquots were frozen in liquid nitrogen and stored at −80 °C. The protein concentration was determined by using the Reducing agent Compatible/Detergent Compatible (RC/DC) Protein Assay (Bio-Rad) following the manufacturer's instructions.

Full-length SNG1 cDNA was amplified from an *A. thaliana* cDNA library (kindly provided by Dr. Hans Sommer, Max Planck Institute for Plant Breeding Research) using the primers F340 (forward, 5′-ATG GTC TCG AGC ATA AAG TTT CTG CTT CTG CTT G-3′) and F341 (reverse, 5′-TTT CTG CAG TTA CAG GGG TTG GCC ACT GAT CCA C-3′). The fragment was cloned into the cloning vector pFK26 (16) using the XhoI and PstI restriction sites, resulting in pFK56. The 35S::SNG1::terminator cassette was excised from pFK56 with XbaI and EcoRI and shuttled into pTP5 (16). The resulting binary vector pFK68 was transformed into *Agrobacterium tumefaciens* strain GV3101 pMP90 (17). Transient overexpression of SNG1 was achieved by co-infiltrating cultures of *Agrobacterium* strains carrying pFK68 together with cultures carrying silencing inhibitor p19 (18) in fully expanded leaves of 4-week-old *Nicotiana benthamiana*. Leaves were harvested after 3 days, and the proteins were extracted as described above.

Infection with B. cinerea—Expanded rosette leaves of 4-week-old wild-type and *pad3* (19) mutant *Arabidopsis* plants were inoculated with 6-μl droplets of either water or 10^6 *B. cinerea* spores/ml (20). Inoculated plants were kept in trays with transparent covers to maintain high humidity and grown under standard conditions in a growth chamber. Inoculated leaves were harvested at 5 days postinfection (dpi) and ground in water as described above.

Activity-dependent Labeling—Small scale activity-dependent labeling reactions with FP were performed in a 50-μl format at a final protein concentration of 1.5 mg/ml in the appropriate 1× buffer (25 mM sodium acetate for pH < 6 or 50 mM Tris for pH = 7 and above). The final concentration of FP used in each labeling reaction was 2 μM. After 1-h incubation at room temperature the labeling reaction was stopped by adding 50 μl of 2× gel loading buffer and heating at 90 °C for 10 min. The samples were then briefly centrifuged (1 min at 16,000 × *g* at room temperature), and 35–50 μl of the supernatant was loaded on a 10% denaturing protein gel and separated by electrophoresis at 250 V for 3.5 h. Labeled proteins were in-gel visualized by fluorescence using a Hitachi FMBio IIe flatbed laser-induced fluorescence scanner (MiraiBio).

MudPIT Sample Preparation and On-bead Digestion—Large scale activity-dependent labeling reactions for MudPIT experiments were performed in 1-ml final volume at a protein concentration of 1.5 mg/ml in 1× PBS with either 5 μl of a 1 mM FPpBio (5 μM FPpBio final) or 5 μl of DMSO (negative control) at room temperature for 2 h. Membranes were solubilized with 100 μl of 10% Triton X-100 (0.9% final concentration) and incubated at 4 °C for 1 h more.

Labeled proteins were affinity-purified as follows. The reaction solution was diluted with 1.4 ml of 1× PBS, briefly vortexed, and applied to a pre-equilibrated PD-10 column (Amersham Biosciences catalog number 17-0851-01). The flow-through was discarded. Proteins were eluted from the column with 3.5 ml of 1× PBS. The desalted protein solution was mixed with 184 μl of 10% SDS and heated at 90 °C for 8 min to denature and unfold proteins. The solution was diluted with 5 ml of 1× PBS. Biotinylated proteins were captured by adding 100 μl of a 50% avidin-Sepharose matrix (prewashed three times with 1× PBS) (Sigma catalog number A9207) and incubated at room temperature for 1 h. The avidin beads were collected by centrifugation (4.5 min at 11,000 rpm) and washed successively two times with 10 ml of 1% SDS, two times with 10 ml of 6 M urea, and finally two times with 10 ml of 1× PBS.

The affinity beads were resuspended in 160 μl of 6 M urea, and captured proteins were first reduced with tris(2-carboxyethyl)phosphine (11 mM; 25 min at 22 °C) and then alkylated with iodoacetamide (13.5 mM; 25 min at 22 °C in the dark). The reaction solution was discarded, and the beads were resuspended in 400 μl of 1 M urea in 1× PBS supplemented with 5 mM $CaCl_2$ and 1.3 ng/μl trypsin (Promega catalog number V511A). The suspension was vigorously shaken at 37 °C for 16 h. The on-bead digestion was stopped by adding 25 μl of 100% formic acid (Acros Organics catalog number 147932500). The reaction solution was cleared by centrifugation (5 min at 16,000 × *g* at room temperature), and the supernatant was transferred into a fresh 1.5-ml tube (Beckman catalog number 357448). Samples were stored at −80 °C until analysis by mass spectrometry. Sample peptides were loaded onto a custom-made biphasic column of a desalting column followed by a separating column (21) Separating columns (100-μm inner diameter, 365-μm outer diameter fused silica capillary tubing (Polymicro Technology)) were generated to have a 5-μm tip using a CO_2 laser puller (Sutter Instrument P-2000 CO_2 laser puller (Novato, CA)). Separating columns were packed with 10 cm of Aqua 5-μm C_{18} (Phenomenex) slurry followed by 3 cm of SCX slurry (Whatman). Desalting columns (250-μm inner diameter, 365-μm outer diameter fused silica capillary tubing (Polymicro Technology)) were packed with 3 cm of Aqua 5-μm C_{18}. Both the separating and desalting column were equilibrated into an aqueous buffer (Buffer A: 95% H_2O, 5% acetonitrile, 0.1% formic acid). Peptides were loaded onto the equilibrated desalting column, and Buffer A was run through the desalting column for 5 min. Finally the separating column was attached in tandem to the separating column. Peptides were analyzed in a five-step MudPIT experiment where the ammonium acetate concentration (0, 25, 50, 80, and 100%) was gradually increased to elute peptides from the SCX column into the C_{18} resin followed by an organic gradient to elute the peptides from the C_{18} resin in the mass spectrometer for analysis (22).

In-gel Digestion—Affinity purification of hydrolases labeled with TriFP was carried out in the same way as described above except that beads were washed six times with 1% SDS. The beads were then resuspended in 50 μl of 2× gel loading buffer supplemented with 5 μl

of 1 M fresh DTT and heated at 90 °C for 5–6 min. Eluted biotinylated hydrolases were separated on a 10% acrylamide gel by electrophoresis (3.5 h at 250 V). Labeled proteins were in-gel visualized by fluorescence scanning. The gel was superimposed onto the obtained printout, and fluorescent gel bands were excised with a razor blade and placed in a 1.5-ml tube. The slices were washed twice with 500 μl of 100 mM ammonium bicarbonate (Sigma catalog number A6141) for 15 min. Proteins were reduced with 200 μl of 10 mM tris(2-carboxyethyl)phosphine (Sigma catalog number 98284) at 62 °C for 30 min and alkylated with 200 μl of 55 mM iodoacetamide (Sigma catalog number I1149) in the dark at 22 °C for 30 min. The gel slices were washed 3 × 15 min in 50:50 acetonitrile, 100 mM ammonium bicarbonate and twice in 50 μl of 100% acetonitrile to dry the gel slices. Acetonitrile was removed, and the slices were dried in a SpeedVac (Savant DNA120 SpeedVac Concentrator, Thermo Electron Corp.). The dried gel slices were incubated with 20 μl of 25 mM ammonium bicarbonate containing 10 ng/μl trypsin (Promega catalog number V511A) for 10 min. The slices were covered with 25 mM ammonium bicarbonate, briefly vortexed, and incubated for 12–16 h at 37 °C under vigorous shaking. The supernatant was transferred to a new tube, and the gel slices were incubated with 5% formic acid (Acros Organics catalog number 147932500) for 15 min at 22 °C and extracted three times with 100% acetonitrile for 5 min. The supernatants were combined with the overnight digestion and concentrated in a SpeedVac to a final volume of 10 μl. The peptide mixture was then loaded onto a custom-made column. Columns (100-μm inner diameter, 365-μm outer diameter fused silica capillary tubing (Polymicro Technology)) were packed with 10 cm of Aqua 5-μm C_{18} (Phenomenex) slurry and finally equilibrated into Buffer A.

Mass Spectrometry—Experiments were performed on a Thermo Linear Trap Quadrupole (LTQ) XL mass spectrometer that was coupled to a Quaternary Agilent 1200 Series pump where the flow was split (0.1 ml/min split to 200 nl/min) before the analytical column. The LTQ XL mass spectrometer was operated using Xcalibur software (version 2.4). The mass spectrometer was set in the positive ion mode, survey scanning between *m/z* of 400 and 1800, with an ionization potential of 2.72 kV. Peptides were separated using either a single reverse phase C_{18} column (gel spots; as described above) or a biphasic C_{18} SCX column and analyzed using a repeating cycle consisting of a full survey scan (3.0×10^4 ions) followed by seven product ion scans (1.0×10^4 ions) where peptides are isolated based on their intensity in the full survey scan (threshold of 1000 counts) for tandem mass spectrum (MS^2) generation that permits peptide sequencing and identification. CID collision energy was set to 35% for the generation of MS^2 spectra. During MS^2 data acquisition dynamic ion exclusion was set to 60 s with a list of excluded ions consisting of 300 members maximum.

Peptide and Protein Identification—The MS^2 spectra data were extracted using RAW Xtractor (version 1.9.1), which is publicly available. MS^2 spectra data were searched using the SEQUEST algorithm (version 3.0) (23) against a custom-made database containing *A. thaliana* sequences from the TAIR8_pep_20080412 database (version April 2008, 32,825 entries) and *B. cinerea* sequences from database botrytis_cinerea_1_proteins (version July 2008, 16,448 entries) that were concatenated to a decoy database in which the sequences for each entry in the original database were reversed. In total the search database contained 98,546 protein sequence entries (49,273 real sequences and 49,273 decoy sequences). SEQUEST searches allowed for oxidation of methionine residues (16 Da), static modification of cysteine residues (57 Da; due to alkylation), no enzyme specificity, and a mass tolerance set to ±1.5 Da for precursor mass and ±0.5 Da for product ion masses. The resulting MS^2 spectra matches were assembled and filtered using DTASelect (version 2.0.27). Spectral matches were retained with Xcorr and ΔCn values that produced a maximum peptide false positive rate of 0.005, calculated from the frequency of matches to the decoy reverse database (24, 25). For each MudPIT analysis, the peptide false positive rate was calculated by dividing hits to the decoy database, multiplied with 100, by the hits to the forward database (summarized at the bottom of supplemental Table S1). For this analysis, tryptic, half-tryptic, and non-tryptic peptides were each individually evaluated using the DTASelect (version 2.0.27) software. In our data set the identification of non-tryptic peptides included half-tryptic peptides from the N and C termini of the identified proteins. Other non-tryptic peptides (14 in the MudPIT analysis) that were identified may represent endogenous activities of cellular proteases or peptides generated by in-source fragmentation. Finally protein identification required the matching of at least two peptides per protein not shared with any other unrelated protein in the database (matches to isoforms coming from the same gene locus were allowed). All peptide data are available as supplemental Tables S3 (MudPIT) and S4 (in-gel digestion).

MudPIT Quantification Using Spectral Counts—The spectral count information stored in the DTAselect-filter.txt files was extracted by using the Perl script dtarray2.pl. The resulting dtarray2.txt file was loaded into Excel (Microsoft Corp.) and further ordered. The number of unique peptides was determined using a custom made Perl script. Proteins with less than two unique peptides were not further analyzed. In cases where several isoforms of a protein were reported only the isoform with highest spectral count value was kept. The spectral counts from the five independent experiments for one protein entry treated with FP or treated with DMSO were summed up. The remaining proteins were divided into four groups depending on the number of times they were observed in independent MudPIT runs. True FP targets were defined as proteins with spectral counts in at least three of five FP-treated samples and in none of the no-probe controls. Proteins found less than three times but that were only found in the FP-treated sample were considered putative FP targets. Proteins with spectral counts in the DMSO-treated samples were considered to be background proteins (supplemental Table S1). The matching PFAM family for each protein was independently determined using a Web-based interface with the default settings (26).

Phylogenetic Trees/Reconstruction—To recreate the phylogenetic trees for S8 (27), S9 (28), S10 (29), carboxylesterase (CXE) (30), and methylesterase (MES) (31) the published gene identifiers were used to extract the respective sequences from the TAIR8_pep_20080412.FASTA database. Sequences from other organisms and sequences from pseudogenes were excluded. The full-length sequences were loaded into ClustalX2.09 (32) and aligned following the guidelines in Hall (33). The unrooted consensus tree from 1000 bootstrap trees was then generated, and the resulting file was exported to Adobe Illustrator for further editing. The alignment files as well as the fully annotated trees are provided as supplemental Figs. S2 and S3. Sequences for calculating the phylogenetic trees of GDSL lipases and pectin acetylesterases were retrieved using the sequences from the identified FP targets. A list of homologous proteins was generated by searching homologous protein sequences using BLASTP against the TAIR8 protein database. Entries with E-value >10–50 were removed to obtain a list of highly homologous proteins. Unique sequence tags were extracted with a custom-made Perl script, and the phylogenetic trees were calculated as described above.

RESULTS

Characterization of FP Labeling—In these studies we used four FP probes that differ only in the linker and reporter tags (Fig. 1*A* and supplemental Fig. S1). The linker is either a hydrophobic C_9 hydrocarbon linker or a hydrophilic C_8O_4

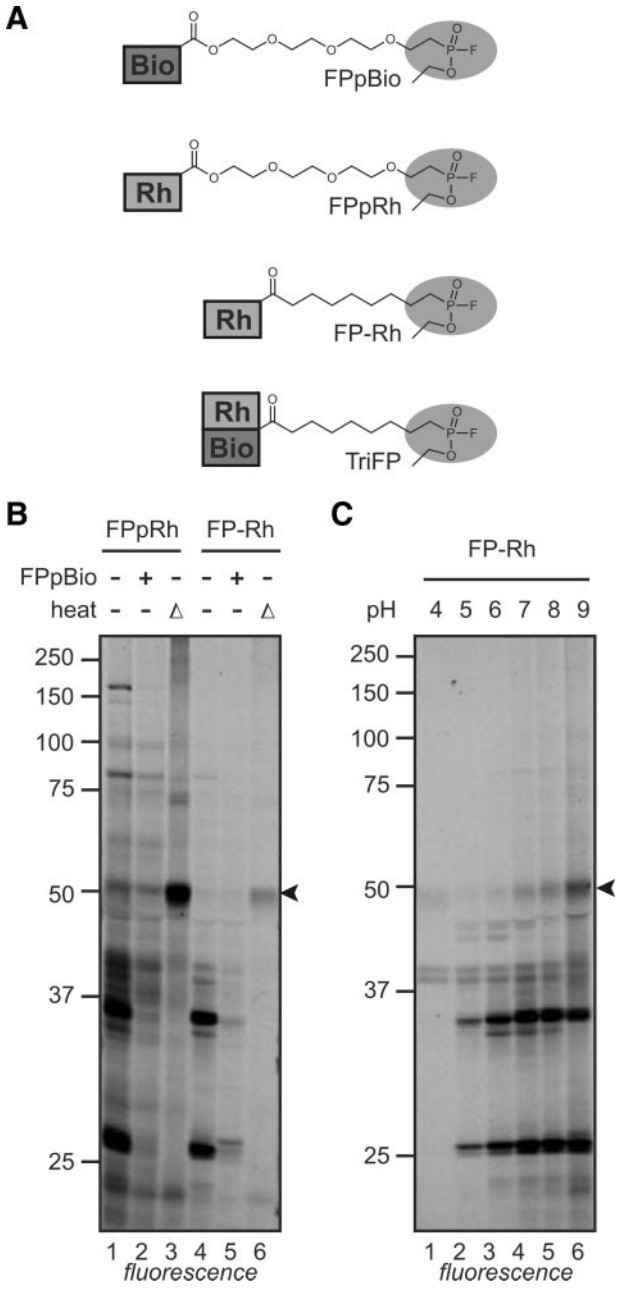

FIG. 1. **FP labeling of *Arabidopsis* leaf extracts.** *A*, structures of the activity-based probes used in this study. All carry an FP reactive group, and some have a PEG (*p*) linker or hydrocarbon linker and either Bio or Rh reporter tags or both (TriFP). Complete structures are given in supplemental Fig. S1. *B*, comparison of labeling with FP with and without PEG linker. *Arabidopsis* leaf extracts were preincubated with or without 20 μM FPpBio or preheated (10 min at 90 °C) and labeled with 2 μM FPpRh or FP-Rh for 2 h. Proteins were separated on large protein gels, and fluorescent signals were detected by fluorescence scanning. *C*, FP labeling profile is pH-dependent. *Arabidopsis* leaf extracts were labeled with FP-Rh at various pH values and analyzed on protein gels by fluorescence scanning. *Arrow*, Rubisco.

polyethylene glycol (PEG; p) linker, which makes the probe more water-soluble (6). The reporter tag is either biotin (Bio) for affinity purification or rhodamine (Rh) for fluorescence detection. The trifunctional TriFP probe contains Bio, Rh, and FP functional groups (13).

We first compared the labeling profiles of the FPpRh and FP-Rh probes. *Arabidopsis* leaf extracts were labeled with FPpRh or FP-Rh, and labeled proteins were detected on protein gels by fluorescence scanning. Both FPpRh and FP-Rh caused similar labeling profiles with strong signals at 26 and 36 kDa and a number of weaker signals at 40 kDa (Fig. 1*B*, *lanes 1* and *4*). However, labeling with FPpRh resulted in stronger signals, especially at high molecular mass with clear signals at 80, 100, and 170 kDa. Labeling of these proteins was suppressed if the proteome was pretreated with an excess of FPpBio or heat-inactivated (Fig. 1*B*, *lanes 2*, *3*, *5*, and *6*), indicating that labeling with FPpRh or FP-Rh is specific and dependent on protein activities.

The above experiment was performed at pH 8. Because protein activities depend on pH, we tested labeling of *Arabidopsis* leaf extracts at various physiological pH values. This revealed that the labeling of each signal has its own pH optimum (Fig. 1*C*). For example, proteins at 45 kDa were only labeled at pH 5 and 6, whereas proteins at 26 and 36 kDa were most strongly labeled at pH8. pH dependence is a hallmark for activity-dependent labeling because it reflects that each enzyme has its own pH-dependent activity.

Identification of FP-labeled Proteins—We followed two approaches to identify FP-labeled proteins (Fig. 2). We first analyzed the full content of FP-labeled proteins using MudPIT (34). The second approach was to identify FP-labeled proteins from 1D protein gels and will be discussed later. MudPIT is based on two-dimensional LC-MS/MS. In this approach, desalted peptide mixtures are first immobilized on a strong cation exchange resin packed in tandem with a reverse phase resin. Peptides are released from the strong cation exchange resin into the reverse phase resin by defined salt plugs. Finally peptides are separated in the reverse phase and eluted into the mass spectrometer for analysis using an organic gradient.

To analyze FP-labeled proteins, *Arabidopsis* rosette extracts were labeled with FPpBio and purified on avidin beads. These beads were stringently washed with SDS and urea, and the immobilized proteins were on-bead digested with trypsin. Eluted peptide mixtures were analyzed by MudPIT. The generated MS data were matched to a database containing 32,825 *Arabidopsis* and 16,448 *B. cinerea* protein sequences (see "Experimental Procedures"). The reverse databases of *Arabidopsis* and *Botrytis* proteins were included in these searches to serve as a negative control (decoy) and to estimate the false positive rate. Proteins with at least two independent peptides identified from the combined database were reported by the search engine. This procedure was performed with five independent FPpBio-labeled extracts and five DMSO-treated negative controls. Only six of the 3000 peptides matched the decoy database (supplemental Table S3).

A total of 163 proteins were above these quality criteria in 10 MudPIT experiments. Three proteins were identified in the

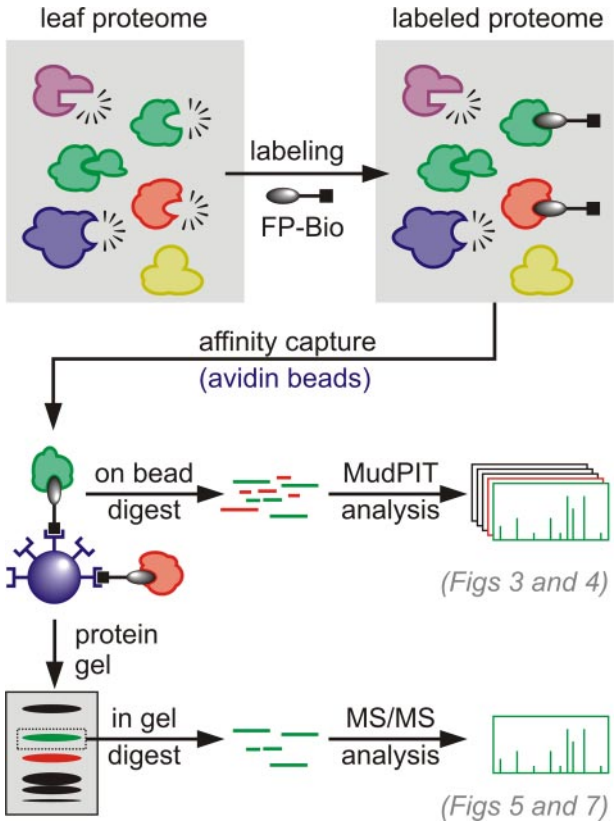

FIG. 2. **Two routes for identifying FP targets.** Biotinylated proteins were purified from FP-labeled proteomes (*top*) using avidin beads. These proteins were subjected to either on-bead trypsin digestion and MudPIT analysis (*middle*) or separated on protein gels and subjected to in-gel trypsin digestion followed by MS/MS analysis (*bottom*).

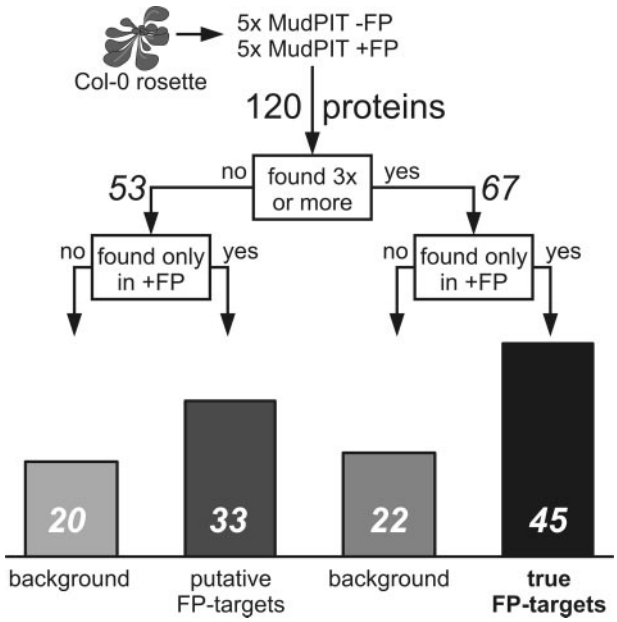

FIG. 3. **Classification of FP-labeled proteins by MudPIT.** Proteins purified after incubation with FPpBio or DMSO were identified by MudPIT and separated into different classes depending on how many times these proteins were identified in independent labeling experiments. The 45 true FP targets were analyzed further in Fig. 4.

decoy database; 160 proteins were *Arabidopsis* proteins. Proteins with fewer than two unique peptides were removed. The remaining 120 *Arabidopsis* proteins were divided into four classes based on their distribution over the MudPIT runs (Fig. 3). Proteins that were identified in only one or two MudPIT runs or with less than 21 spectral counts were not further analyzed. Of these 53 proteins, 33 were only found in FPpBio-labeled samples, and many of those are putative serine hydrolases (see supplemental Table S1).

Of the 120 identified *Arabidopsis* proteins, 67 were identified in three or more MudPIT experiments. Of these, 22 proteins were found in both the FPpBio-labeled sample and DMSO control with similar spectral counts and were considered to be background proteins. These proteins include the small and large subunits of Rubisco (At1g67090 and AtCg00490, respectively) and protein P of photosystem II (PsbP, At1g06680), which are highly abundant proteins in a leaf proteome. Among the background proteins we also found (3-methylcrotonyl)-CoA carboxylase (At1g03090), acetyl-CoA carboxylase (ACC1, At1g36160), and biotin carboxyl carrier proteins (BCCP1, AT5G16390; and BCCP2, At5g15530), which are all endogenously biotinylated proteins, explaining their purification on avidin columns.

The remaining 45 *Arabidopsis* proteins were identified at least three times with over 20 spectral counts but only in the FPpBio-labeled samples. These proteins are summarized in Fig. 4. Significantly, all of these 45 proteins are Ser hydrolases carrying a nucleophilic Ser residue in their active site center (Table I). However, the enzymatic functions of these enzymes are remarkably different (Fig. 4 and Table I). In total we identified six subtilases (family S8, clan SB), four prolyl oligopeptidases-like proteins (POPLs, family S9, clan SC), 12 serine carboxypeptidase-like proteins (SCPLs, family S10, clan SC), nine pectin acetylesterase-like proteins, five GDSL-like lipases, five CXEs, two MESs, and two other Ser hydrolases. These Ser hydrolases belong to 10 different protein families, indicated with differently colored domains in Fig. 4*C* and summarized in Table I. Seven of these protein families belong to the α/β-hydrolases (clan CL0028), which have a catalytic triad in the order of Ser-Asp-His (Table I).

Only nine of these 45 *Arabidopsis* serine hydrolases have been characterized previously. These are proteases ARE12, TPP2, AARE, and BRS1; esterases CXE12, MES2, and MES3; SNG1; and SFGH (explained in legend of Fig. 4*C*). Their biochemical and biological activities are very diverse and are summarized in the "Discussion."

To investigate which of the Ser hydrolases are represented in our analysis, we constructed genome-wide phylogenetic trees for each of the families and marked them with the identified enzymes (Fig. 4*D* and supplemental Fig. S2). This analysis revealed that the relative representation differs between the enzyme families. For example, we identified nearly

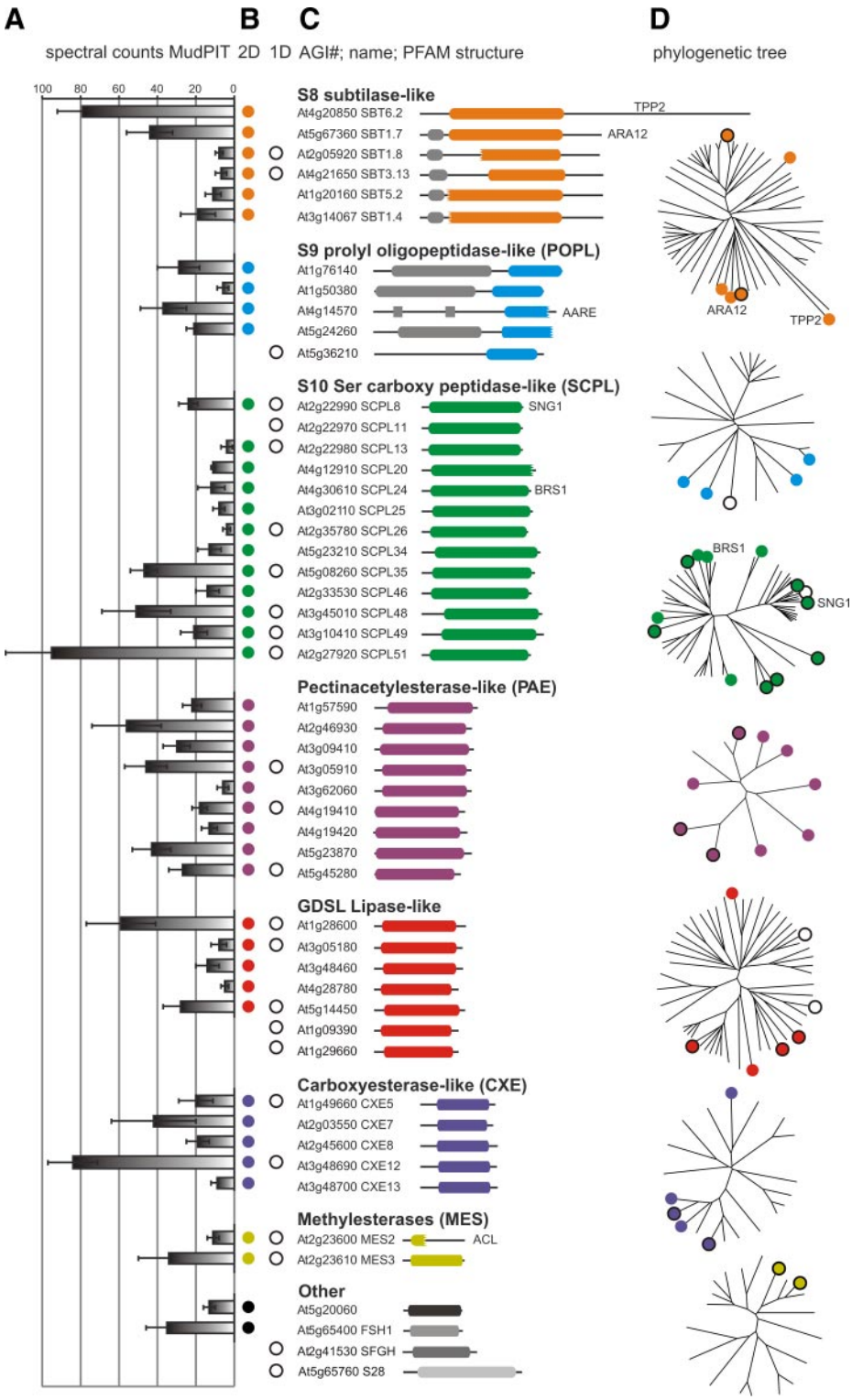

FIG. 4. **Analysis of the Ser hydrolases identified by MudPIT and from protein gels.** *A*, spectral counts in the MudPIT analysis. The S.E. is calculated over all five independent FP labeling experiments. *B*, proteins that were identified by MudPIT (two-dimensional (*2D*)) and from 1D protein gel (Fig. 7) are indicated with *filled* and *open circles*, respectively. *C*, identities of the FP-labeled proteins. The *Arabidopsis* Genome Initiative (*AGI*) code for each of the identified protein is followed by the common names and a PFAM-predicted structure. *D*, the identified proteins represent different subclasses in each of the phylogenetic threes. Phylogenetic trees were constructed for each of the subfamilies (see supplemental Fig. S2). The *circles* indicate the proteins that were identified as FP-labeled proteins: *closed*, found in MudPIT; *bordered*, found on 1D gel. *SFGH*, *S*-formylglutathione hydrolase; *SBT*, subtilase; *TPP2*, tripeptidyl peptidase-2; *AARE*, acylamino acid releasing enzyme; *POPL*, prolyl oligopeptidase-like; *SCPL*, serine carboxypeptidase-like; *SNG1*, sinapolyglucose accumulator-1; *BRS1*, Bri1 suppressor-1; *PAE*, pectineacetylesterase; *CXE*, carboxyesterase; *MES*, methylesterase; *ACL*, acetone cyanohydrin lyase; *FSHI*, family of serine hydrolases-I.

all pectin acetylesterases and many SCPLs but only a few subtilases or POPLs. Within each of these enzyme families, however, the distribution of the identified proteins is not clade-specific, which is consistent with the non-selective, broad reactivity of FP toward Ser hydrolases (5).

Comparison with gene expression data from the Mass Parallel Serial Sequencing database and Genevestigator revealed that the identified Ser proteases are a subset of the expressed Ser hydrolases (data not shown). The absence of many of the expressed Ser hydrolases in our FP labeling indicate that

TABLE I
Protein families identified by FP labeling

Enzymes[a]	At[b]	Bc[b]	PFAM	Structural clan	Catalytic residues[c]
Subtilase	6	0	PF00082	None	Asp-His-**Ser**
POPL	5	0	PF00326	CL0028: α/β hydrolase	**Ser**-Asp-His
SCPL	12	1	PF00450	CL0028: α/β hydrolase	**Ser**-Asp-His
PAE	9	0	PF03283	None	**Ser**-Asp-His
Lipase	7	2	PF00657	CL0264: SGNH hydrolase	**Ser**-Gly-Asn-His
CXE	5	0	PF07859	CL0028: α/β hydrolase	**Ser**-Asp-His
MES	3	0	PF00561	CL0028: α/β hydrolase	**Ser**-Asp-His
At5g20060	1	0	PF02230	CL0028: α/β hydrolase	**Ser**-Asp-His
FSH1	1	0	PF03959	CL0028: α/β hydrolase	**Ser**-His-Asp
SFGH	1	0	PF00756	CL0028: α/β hydrolase	**Ser**-Asp-His
S28	1	0	PF05577	CL0028: α/β hydrolase	**Ser**-Asp-His
Cutinase	0	2	PF01083	CL0028: α/β hydrolase	**Ser**-Asp-His
Lactamase	0	1	PF00144	CL0013: β-lactamase	**Ser**-Asp-His
Total	51	6	14	5	All Ser

[a] Abbreviations as in the legend of Fig. 4*C*.
[b] Number of individual enzymes identified from *A. thaliana* (At) and *B. cinerea* (Bc).
[c] Bold, catalytic serine residue.

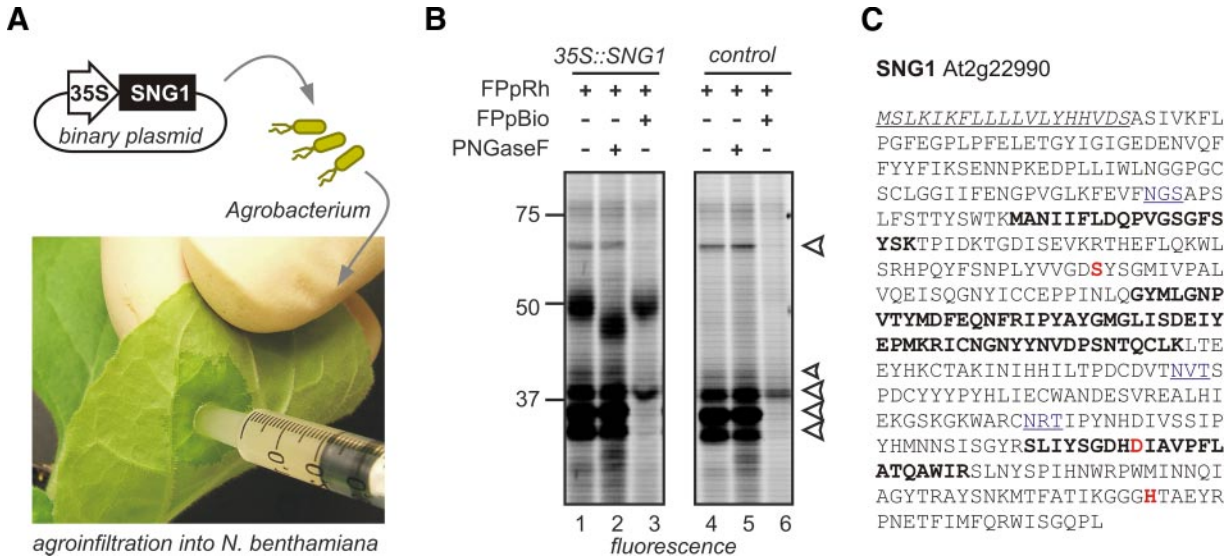

FIG. 5. **Detailed analysis of SNG1.** *A*, overexpression of SNG1 by agroinfiltration. SNG1 was cloned into an overexpression vector and transformed into *A. tumefaciens*. *Agrobacterium* cultures were infiltrated into leaves of *N. benthamiana* together with cultures carrying the p19 silencing suppressor. Extracts were generated at 5 days after agroinfiltration and used for FP labeling. *B*, specific labeling of agroinfiltrated SNG1. Extracts from agroinfiltrated leaves expressing SNG1 with silencing suppressor p19 or p19 alone were preincubated with or without 20 μM FPpBio and labeled with 2 μM FPpRh. FP-labeled extracts were treated with or without peptide-*N*-glycosidase F (*PNGaseF*), separated on a protein gel, and detected using fluorescence scanning. *Open arrows* indicate FP targets of *N. benthamiana*. *C*, peptides identified from SNG1. A tryptic digest of FP-labeled SNG1 isolated from gel was analyzed by MS. *Underlined italics*, signal peptide; *bold*, identified peptides; *underlined blue*, putative *N*-glycosylation sites; *bold red*, catalytic residues.

these enzymes were (i) not active under the tested conditions, (ii) not abundant enough to be detected, or (iii) not reacting with the FP probe.

Taken together, FP labeling enables the detection of a diverse range of Ser hydrolase activities in *Arabidopsis*. The fact that each of these enzymes reacts with FP in leaf extracts demonstrates that their active site is accessible and reactive toward FP, indicating that these enzymes are active.

FP Labeling of Agroinfiltrated SNG1—To confirm and study FP labeling of one of the enzymes further, we selected SNG1. SNG1 is a plant-specific acyltransferase that was previously studied biochemically and shown to act in the production of sinapoylmalate in *Arabidopsis* leaves (11). To produce SNG1 *in planta*, we cloned the open reading frame into a binary expression vector and overexpressed it in *N. benthamiana* through agroinfiltration (Fig. 5*A*; Refs. 18 and 35). FPpRh labeling of extracts from leaves producing SNG1

revealed that there is an additional 50-kDa signal that was absent in the control (Fig. 5*B*, *lanes 1* and *4*). Five additional signals were also present in the control and are probably derived from *N. benthamiana* or *A. tumefaciens* (Fig. 5*B*, *lane 4*).

Because the protein size is larger than expected and SNG1 carries three putative *N*-glycosylation sites (Fig. 5*C*), we tested whether SNG1 was *N*-glycosylated. Deglycosylation using peptide-*N*-glycosidase F caused a shift of the SNG1-specific signal to 45 kDa (Fig. 5*B*, *lane 2*), which is close to the predicted and observed molecular mass of mature SNG1 (11). Other signals did not shift, indicating that these are not *N*-glycosylated proteins (Fig. 5*B*, *lanes 2* and *5*). Preincubation with an excess of FPpBio prevents labeling of most of the signals but only partially suppresses labeling of the SNG1-specific signal and the 37-kDa signal (Fig. 5*B*, *lanes 3* and *6*), which is presumably because of the high abundance of these proteins and a lower affinity toward FPpBio compared with other FP targets.

To confirm that the additional signal represents SNG1, we labeled SNG1-containing extracts with TriFP, purified biotinylated proteins, and subjected the 50-kDa signal to trypsin digestion and LC-MS/MS. This yielded six SNG1-specific peptides (30 spectral counts; sequence coverage, 22%), demonstrating that this signal indeed represents SNG1 (Fig. 5*C* and supplemental Table S5). Peptides carrying the putative *N*-glycosylation site and the active site Ser residue were not annotated probably because they are modified by *N*-glycosylation and FP labeling, respectively.

Ser Hydrolase Activities during Fungal Infection—To apply FP profiling, we investigated changes in Ser hydrolase activities during infection with the necrotrophic fungal pathogen *B. cinerea*. *Botrytis* can penetrate healthy undamaged tissues of a wide range of plants and fruits and causes severe losses in the grape and fruit industry (36). *Arabidopsis* plants are well protected against *Botrytis* through the inducible production of phytoalexins like camalexin. Phytoalexin-deficient mutant *pad3* carries a mutation in CYP71B15, which catalyzes the last step in camalexin biosynthesis (37, 38). The absence of camalexin production in *pad3* mutant plants explains their susceptibility for *Botrytis* infection (19). To investigate Ser hydrolase activities during infection with *Botrytis*, we infected wild-type and *pad3* mutant *Arabidopsis* plants with *Botrytis* and performed FP profiling on extracts taken at different days post-infection (dpi). This analysis revealed no changes in the FP profile during the first 3 days, consistent with the 3-day latent period of *Botrytis* infection (Fig. 6). At 4 and 5 dpi, the 25-kDa signal became weaker in *Botrytis*-infected leaves (Fig. 6). This process was faster in *pad3* mutants than in wild-type plants. At 5 dpi a number of additional signals appeared in the *pad3* mutant. At this stage, half of the *Botrytis*-infected leaves of the *pad3* mutant were macerated, whereas the infection in wild-type plants did not progress beyond the site of the inoculation (Fig. 7*A*).

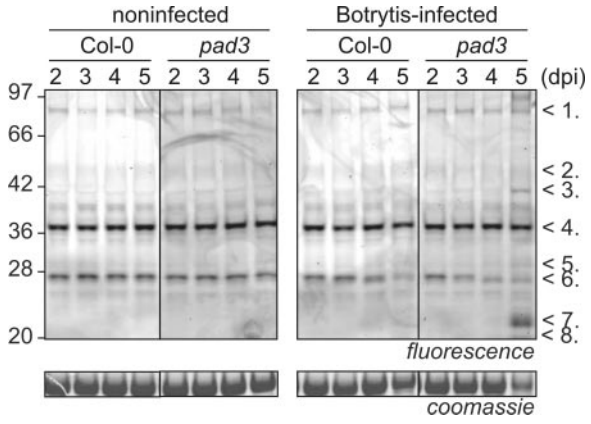

FIG. 6. **Ser hydrolase activities during the *Arabidopsis-Botrytis* interaction.** *Arabidopsis* wild type (Col-0) and *pad3* mutant were infected with droplets containing *B. cinerea* spores. Leaf extracts were labeled with FPpRh at different dpi, and fluorescent proteins were detected on protein gels. Eight bands (*1–8*) indicated on the *right* are analyzed in Fig. 7.

To identify the enzymes causing the signals in these profiles, we labeled extracts of *Botrytis*-infected wild-type and *pad3* mutant plants taken at 5 dpi with TriFP and purified the biotinylated proteins. The profile of the purified TriFP-labeled sample contained signals in eight regions that correspond with the time course (compare Fig. 7*B* with Fig. 6; regions are numbered *1–8*). Many regions contained multiple Ser hydrolases and background proteins (listed in supplemental Table S2). Ser hydrolases with the highest spectral counts are summarized in Fig. 7*C*. The size of the open reading frames corresponds to the position of the protein in the profile (Fig. 7*E*).

The Col-0 sample consists almost entirely of *Arabidopsis* enzymes (see below), whereas the *pad3* sample also contains several *Botrytis* enzymes (Fig. 7*C*, indicated in *bold*). Signals in regions 3, 7, and 8 in the *pad3* mutants were caused by *Botrytis*-derived enzymes. A *Botrytis* lactamase and a *Botrytis* SCPL caused the signal in region 3, and two cutinases caused the signal in regions 7 and 8. Both lactamases and the cutinases are Ser hydrolases and represent additional PFAM families (Table I).

The spectral counts of the *Arabidopsis* Ser hydrolases (Fig. 7*D*) correspond to the signal intensities of the profile (Fig. 7*B*). For example, signals in regions 1 and 2 were caused by prolyl oligopeptidase At5g36210 and SNG1, respectively (Fig. 7*C*). The reduced spectral counts and fluorescent signals (Fig. 7, *B* and *D*) suggest that both enzymes have a reduced activity in infected *pad3* mutants when compared with infected Col-0 plants. Furthermore the down-regulated signal in region 6 was likely caused by reduced activities of methylesterases MES2 and MES3 (Figs. 5 and 7, *B* and *D*). In contrast, *S*-formylglutathione hydrolase activity causing signals in region 5 was up-regulated in *pad3* when compared with Col-0 (Fig. 7, *B* and *D*). Region 4 consists of multiple bands and multiple *Arabidopsis* Ser hydrolases. Some of these hydrolases such

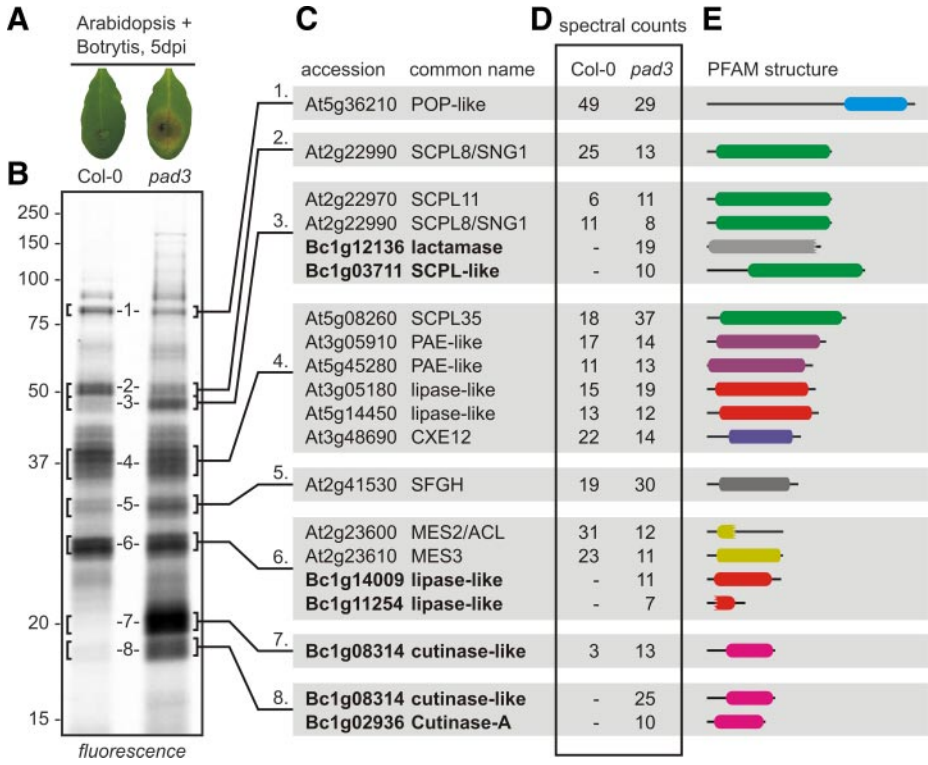

FIG. 7. **Identities of Ser hydrolases during the *Arabidopsis-Botrytis* interaction.** *A*, symptoms of *Botrytis*-infected *Arabidopsis* leaves at the time of analysis. Leaves of wild-type (Col-0) and *pad3* mutant plants were infected with *Botrytis* using a spore-containing droplet. The picture was taken at 5 dpi. *B*, profile of purified TriFP-labeled proteins of *Botrytis*-infected tissues at 5 dpi used for identification. Protein extracts were labeled with TriFP, and biotinylated proteins were purified and separated on a protein gel. 16 fluorescent bands from eight regions (*1–8*) were excised and digested with trypsin, and eluted peptides were analyzed by LC-MS/MS. *C*, Ser hydrolases identified from the eight regions. *Botrytis* proteins are indicated in *bold*. *D*, spectral counts of each identified Ser hydrolase from the Col-0 and *pad3* samples. *E*, PFAM structure of each identified Ser hydrolase using the same colors as in Fig. 4. New PFAM structures are cutinases (*pink*) and lactamases (*light gray*). For protein abbreviations see legend of Fig. 4*C*.

as SCPL35 and CXE12 might be differentially active between Col-0 and *pad3*. Thus, FP profiling revealed a series of Ser hydrolase activities that change during *Botrytis* infection. It seems likely that these Ser hydrolase activities play a role during the *Botrytis-Arabidopsis* interaction.

DISCUSSION

We performed ABPP with FP-based probes to identify activities of over 50 *Arabidopsis* and *Botrytis* serine hydrolase activities in (infected) leaf proteomes. These enzymes represent more than 10 different serine hydrolase families and include many proteases, lipases, and esterases.

The fact that only Ser hydrolases were found among FP-labeled proteins in the MudPIT analysis is the result of stringent selection of the MudPIT data and illustrates the selectivity of the FP-based probes for reacting with active serine residues that are part of catalytic triads. This is consistent with previous findings and explains why this probe is used so frequently, *e.g.* to identify differential activities (*e.g.* Refs. 7 and 8), select specific inhibitors (*e.g.* Refs. 9 and 39), or study individual enzymes (*e.g.* Refs. 40 and 41). In general, FP probes having a PEG linker label with stronger intensities and more signals than those with a hydrocarbon linker (Fig. 1*B*). This was also found in animal proteomes and is probably due to the increased water solubility and accessibility of this probe (6).

Phylogenetic analysis showed that not all *Arabidopsis* serine hydrolases were detected. The absence of the other hydrolases can have different reasons. First, many *Arabidopsis* genes are not expressed in leaves or under the conditions tested. This holds, for example, for many genes encoding subtilases (27). Second, some serine hydrolases may not be active under the conditions tested. We showed, for example, that labeling depends on pH (Fig. 1*C*), indicating that many enzymes cannot be labeled at non-optimal conditions. Third, some enzymes might not be abundant enough to be detected. Many of the 33 putative FP targets that were only found once or twice in MudPIT runs (Fig. 3) could belong to this class. Fourth, FP may not react with every serine hydrolase. For example, there are other FP probes available that label different serine hydrolases (42). Differences in labeling profiles between FP-Rh and FPpRh indeed indicate that labeling depends on the probe used. However, most clades within phylogenetic trees were represented, suggesting that there is limited selectivity of the FP probe and that in principle many active serine hydrolases could be labeled by FP.

The diversity of serine hydrolase families detected in this study is striking because we found representatives of 14 different PFAM families (Table I). Most of these hydrolase families were detected previously with FP-based probes (*e.g.* Refs. 7–9 and 39–41), but others like pectin acetylesterases and cutinases were not reported as FP targets before and are plant- and/or pathogen-specific. Most of the FP-labeled hydrolases share the same α/β-hydrolase fold and are probably evolutionary related. However, some serine hydrolases belong to different clades and have different structures. Thus, despite the fact that these proteins belong to different families and have different structures, they can

all carry a catalytic serine residue and can all be labeled with FP-based probes.

Only nine of the 45 detected *Arabidopsis* enzymes were previously characterized functionally and/or biochemically (Fig. 4). ARA12 (SBT1.7) is a secreted subtilase required for the release of mucilage to break the seed coat during germination but with unknown function in leaves (43, 44). TPP2 (tripeptidyl peptidase-II, SBT6.2) is a large oligomeric cytosolic protease that degrades peptides produced by the proteasome (45). Acylamino acid-releasing enzyme acts as a tetrameric protein complex in the chloroplast stroma and regulates the turnover of *N*-acylated proteins through the hydrolysis of the N-terminal N^{α}-acylated amino acids (46). SNG1 (sinapoylglucose accumulator-1, SCPL8) acts as an acyltransferase in the production of sinapoylmalate, which is thought to protect leaves from UV irradiation (11, 47). Overexpression of carboxypeptidase BRS1 (Bri1 suppressor-1, SCPL24) suppresses the dwarfed phenotype of weak *bri1* mutants that are hampered in the perception of the steroid hormone brassinolide (48). CXE12 is a carboxylesterase that hydrolyzes ester bonds in xenobiotics and natural products (49). Methylesterases like MES2 and MES3 can hydrolyze methylsalicylate, methyljasmonate, and methylindoleacetic acid and are thought to play a role in the regulation of these plant hormones (14, 31). Finally, *S*-formylglutathione hydrolase (SFGH) acts as a protein dimer in formaldehyde metabolism by hydrolyzing *S*-formylglutathione, releasing formic acid and glutathione (50).

As summarized above, the detected enzymes represent a diversity of biochemical pathways. However, the biochemical functions of the majority of the detected serine hydrolases are unknown. Some of the detected enzymes might belong to the same biochemical pathway. For example, production of sinapoylmalate involves hydrolysis of sinapine esters and re-esterification to malate. This is mediated by the activities of a GDSL lipase and acyltransferase SNG1, respectively (11, 12). SNG1 was repeatedly detected in our assays, and it is tempting to speculate that one or more of the detected GDSL lipases releases sinapate for sinapoylmalate synthesis.

The annotation of biochemical and biological functions of the detected serine hydrolases requires further functional analysis. This may not be a simple task because many hydrolases belong to large gene families of which members might act redundantly. Methylesterases MES1, -7, and -9, for example, act redundantly in the hydrolysis of methylsalicylate (14). Profiling with FP is a powerful tool to assist in the functional analysis of serine hydrolases, *e.g.* to monitor remaining hydrolase activities in genetically modified *Arabidopsis* plants. FP profiling can also be used to select for specific inhibitors of serine hydrolases. Specific inhibitors can be used in chemical knock-out assays to address the biochemical and biological roles of the targeted hydrolases. Such approach has been successfully applied to annotate *e.g.* the biochemical function of the human serine hydrolase KIAA1363 in lipid metabolism (39).

We analyzed FP-labeled proteomes through both MudPIT and 1D protein gels. Each approach has its advantages and disadvantages. The advantage of MudPIT analysis is the large number of hydrolases that were identified from a single leaf extract. The robustness of MudPIT analysis is reflected in the repeated detection of the same 45 hydrolases in independent MudPIT analyses. The disadvantage of MudPIT is that topological information (size of the protein) is lost, and this method is not suitable for high throughput analysis. In addition, we observed a variation in spectral counts between the different MudPIT experiments that is possibly caused by variation in labeling or analysis and illustrates that a sufficient number of replicates is required for quantitative analysis. In contrast, detecting FP-labeled proteins on 1D protein gels supports high throughput quantitative analysis and provides topological information. A disadvantage of this method, however, is that fewer proteins can be detected and that many signals overlap. The choice of the analysis therefore depends on the application.

We used 1D protein gel analysis to monitor the infection of *Arabidopsis* by *B. cinerea* and provide a first glimpse into the differential hydrolase activities during *Botrytis* infection. Both *Arabidopsis* and *Botrytis* hydrolases were detected in infected *pad3* mutant plants (Fig. 7). *Botrytis* cutinases and lipases are thought to play a key role in *Botrytis* infection process because *Botrytis* infects by dissolving the cuticle (36). However, knock-out strains lacking cutinase *CutA* and lipase *lip1* do not show reduced virulence (51, 52). Our data indicate that CutA is not the dominant cutinase during infection and that at least two *Botrytis* GDSL-like lipases are produced and active during infection. This activity information, combined with the *Botrytis* genome sequence, is essential information for focused strategies to further investigate *Botrytis* pathogenesis.

Several *Arabidopsis* enzymes show differential activities during *Botrytis* infection. For example, spectral counts suggest that activities of methylesterases MES2 and MES3 and of acyltransferase SNG1 were down-regulated, whereas *S*-formylglutathione hydrolase activity increased (Fig. 7). It is unknown whether these effects are mediated by the pathogen to promote infection or mediated by the plant to suppress pathogen invasion. MES2/3 activities, for example, might be down-regulated by *Botrytis* to suppress salicylic acid signaling pathways. SNG1 activity, on the other hand, might be down-regulated to divert metabolic pathways to produce secondary metabolites that are harmful to *Botrytis*. These initial FP labeling experiments illustrate the kinds of questions that are raised by investigating plant-pathogen interactions using ABPP. However, more experiments are required to confirm the differential activities and to reveal their molecular mechanisms and biological functions.

Acknowledgements—We are very grateful to Gabriel Simon (Scripps Research Institute, La Jolla, CA) for help with data management and for providing dtarray2.pl, Melissa Dix (Scripps Research Institute, La Jolla, CA) for help with in-gel digestions, and Dr. Hans

Sommer (Max Planck Institute for Plant Breeding Research, Cologne, Germany) for providing *Arabidopsis* cDNA. We thank all the members of the Cravatt laboratory and of the Van der Hoorn laboratory (Plant Chemetics lab) for helpful discussions.

* This work was supported by the Max Planck Society and Deutsche Forschungsgemeinschaft Project HO 3983/3-3 and HO 3983/4-1.

S The on-line version of this article (available at http://www.mcponline.org) contains supplemental material.

§ Both authors made equal contributions to this work.

** To whom correspondence should be addressed: Tel.: +49-221-5062-245; Fax: +49-221-5062-207; E-mail: hoorn@mpiz-koeln.mpg.de.

REFERENCES

1. The Arabidopsis Genome Initiative (2000) Analysis of the genome sequence of the flowering plant Arabidopsis thaliana. *Nature* **408,** 796–815
2. Cravatt, B. F., Wright, A. T., and Kozarich, J. W. (2008) Activity-based protein profiling: from enzyme chemistry to proteomic chemistry. *Annu. Rev. Biochem.* **77,** 383–414
3. Verhelst, S. H., and Bogyo, M. (2005) Dissecting protein function using chemical proteomic methods. *QSAR Comb. Sci.* **24,** 261–269
4. Kobe, B., and Kemp, B. E. (1999) Active-site-directed protein regulation. *Nature* **402,** 373–376
5. Liu, Y., Patricelli, M. P., and Cravatt, B. F. (1999) Activity-based protein profiling: the serine hydrolases. *Proc. Natl. Acad. Sci. U. S. A.* **96,** 14696–14699
6. Kidd, D., Liu, Y., and Cravatt, B. F. (2001) Profiling serine hydrolase activities in complex proteomes. *Biochemistry* **40,** 4005–4015
7. Jessani, N., Liu, Y., Humphrey, M., and Cravatt, B. F. (2002) Enzyme activity profiles of the secreted and membrane proteome that depict cancer cell invasiveness. *Proc. Natl. Acad. Sci. U. S. A.* **99,** 10335–10340
8. Jessani, N., Humphrey, M., Hayes McDonald, W., Niessen, S., Masuda, K., Gangadharan, B., Yates, J. R., Mueller, B. M., and Cravatt, B. F. (2004) Carcinoma and stromal enzyme activity profiles associated with breast tumor growth in vivo. *Proc. Natl. Acad. Sci. U. S. A.* **101,** 13756–13761
9. Leung, D., Hardouin, C., Boger, D. L., and Cravatt, B. F. (2003) Discovering potent and selective reversible inhibitors of enzymes in complex proteomes. *Nat. Biotechnol.* **21,** 687–691
10. Zhang, D., Saraf, A., Kolasa, T., Bhatia, P., Zheng, G. Z., Patel, M., Lannoye, G. S., Richardson, P., Steward, A., Rogers, J. C., Brioni, J. D., and Surowy, C. S. (2007) Fatty acid amide hydrolase inhibitors display broad selectivity and inhibit multiple carboxylesterases as off-targets. *Neuropharmacology* **52,** 1085–1105
11. Lehfeldt, C., Shirley, A. M., Meyer, K., Ruegger, M. O., Cusumano, J. C., Viitanen, P. V., Strack, D., and Chapple, C. (2000) Cloning of the *SNG1* gene of Arabidopsis reveals a role for a serine carboxypeptidase-like protein as an acyltransferase in secondary metabolism. *Plant Cell* **12,** 1295–1306
12. Clauss, K., Baumert, A., Nimtz, M., Milkowski, C., and Strack, D. (2008) Role of a GDSL lipase-like protein as sinapine esterase in Brassicaceae. *Plant J.* **53,** 802–813
13. Gershater, M. C., Cummins, I., and Edwards, R. (2007) Role of a carboxylesterase in herbicide bioactivation in *Arabidopsis thaliana*. *J. Biol. Chem.* **282,** 21460–21466
14. Vlot, A. C., Liu, P. P., Cameron, R. K., Park, S. W., Yang, Y., Kumar, D., Zhou, F., Padukkavidana, T., Gustafsson, C., Picherski, E., and Klessig, D. F. (2008) Identification of likely orthologs of tobacco salicylic acid-binding protein 2 and their role in systemic acquired resistance in *Arabidopsis thaliana*. *Plant J.* **53,** 445–456
15. Patricelli, M. P., Giang, D. K., Stamp, L. M., and Burbaum, J. J. (2001) Direct visualization of serine hydrolase activities in complex proteomes using fluorescent active site-directed probes. *Proteomics* **1,** 1067–1071
16. Shabab, M., Shindo, T., Gu C., Kaschani, F., Pansuriya, T., Chintha, R., Harzen, A., Colby, T., Kamoun, S., and Van der Hoorn, R. A. L. (2008) Fungal effector protein AVR2 targets diversifying defense-related Cys proteases of tomato. *Plant Cell* **20,** 1169–1183
17. Koncz, C., and Schell, J. (1986) The promoter of Tl-DNA gene 5 controls the tissue-specific expression of chimeric genes carried by a novel type of Agrobacterium binary vector. *Mol. Gen. Genet.* **204,** 383–396
18. Voinnet, O., Rivas, S., Mestre, P., and Baulcombe, D. (2003) An enhanced transient expression system in plants based on suppression of gene silencing by the p19 protein of tomato bushy stunt virus. *Plant J.* **33,** 949–956
19. Ferrari, S., Plotnikova, J. M., De Lorenzo, G., and Ausubel, F. M. (2003) *Arabidopsis* local resistance to *Botrytis cinerea* involves salicylic acid and camalexin and requires EDS4 and PAD2, but not SID2, EDS5 or PAD4. *Plant J.* **35,** 193–205
20. Brouwer, M., Lievens, B., Van Hemelrijck, W., Van den Ackerveken, G., Vammue, B. P. A., and Thomma, B. P. H. J. (2003) Quantitation of disease progression of several microbial pathogens on *Arabidopsis thaliana* using real-time fluorescence PCR. *FEMS Microbiol. Lett.* **228,** 241–248
21. Link, A. J., Eng, J., Schieltz, D. M., Carmack, E., Mize, G. J., Morris, D. R., Garvik, B. M., and Yates, J. R., III (1999) Direct analysis of protein complexes using mass spectrometry. *Nat. Biotechnol.* **17,** 676–682
22. Jessani, N., Niessen, S., Wei, B. Q., Nicolau, M., Humphrey, M., Ji, Y., Han, W., Noh, D. Y., Yates, J. R., III, Jeffrey, S. S., and Cravatt, B. F. (2005) A streamlined platform for high-content functional proteomics of primary human specimens. *Nat. Methods* **2,** 691–697
23. Eng, J. K., McCormack, A. L., and Yates, J. R., III (1994) An approach to correlate tandem mass spectral data of peptides with amino acid sequences in a protein database. *J. Am. Soc. Mass Spectrom.* **5,** 976–989
24. Tabb, D. L., McDonald, W. H., and Yates, J. R. (2002) DTASelect and Contrast: tools for assembling and comparing protein identifications from shotgun proteomics. *J. Proteome Res.* **1,** 21–26
25. Cociorva, D., Tabb, D. L., and Yates, J. R. (2007) Validation of tandem mass spectrometry database search results using DTASelect. *Curr. Protoc. Bioinformatics* 13.4.1–13.4.14
26. Finn, R. D., Tate, J., Mistry, J., Coggill, P. C., Sammut, S. J., Hotz, H. R., Ceric, G., Forslund, K., Eddy, S. R., Sonnhammer, E. L., and Bateman, A. (2008) The Pfam protein families database. *Nucleic Acids Res.* **36,** D281–D288
27. Rautengarten, C., Steinhauser, D., Bussis, D., Stintzi, A., Schaller, A., Kopka, J., and Altmann, T. (2005) Inferring hypotheses on functional relationships of genes: Analysis of the Arabidopsis thaliana subtilase gene family. *PLoS Comput. Biol.* **1,** e40
28. Tripathi, L. P., and Sowdhamini, R. (2006) Cross genome comparisons of serine proteases in Arabidopsis and rice. *BMC Genomics* **7,** 200
29. Fraser, C. M., Rider, L. W., and Chapple, C. (2005) An expression and bioinformatics analysis of the Arabidopsis serine carboxypeptidase-like gene family. *Plant Physiol.* **138,** 1136–1148
30. Marshall, S. D., Putterill, J. J., Plummer, K. M., and Newcomb, R. D. (2003) The carboxylesterase gene family from *Arabidopsis thaliana*. *J. Mol. Evol.* **57,** 487–500
31. Yang, Y., Xu, R., Ma, C., Vlot, A. C., Klessig, D. F., and Pichersky, E. (2008) Inactive methyl indole-3-acetic acid ester can be hydrolyzed and activated by several esterases belonging to the AtMES esterase family of Arabidopsis. *Plant Physiol.* **147,** 1034–1045
32. Larkin, M. A., Blackshields, G., Brown, N. P., Chenna, R., McGettigan, P. A., McWilliam, H., Valentin, F., Wallace, I. M., Wilm, A., Lopez, R., Thompson, J. D., Gibson, T. J., and Higgins, D. G. (2007) Clustal W and Clustal X version 2.0. *Bioinformatics* **23,** 2947–2948
33. Hall, B. G. (2004) *Phylogenetic Trees Made Easy: a How-To Manual*, 2nd Ed., pp. 1–70, Sinauer Assoc., Sunderland, MA
34. Ducret, A., Van Oostveen, I., Eng, J. K., Yates, J. R., and Aebersold, R. (1998) High throughput protein characterization by automated reverse-phase chromatography/electrospray tandem mass spectrometry. *Protein Sci.* **7,** 706–719
35. Van der Hoorn, R. A. L., Laurent, F., Roth, R., and De Wit, P. J. G. M. (2000) Agroinfiltration is a versatile tool that facilitates comparative analysis of *Avr9*/*Cf-9*-induced and *Avr4*/*Cf-4*-induced necrosis. *Mol. Plant-Microbe Interact.* **13,** 439–446
36. Van Kan, J. A. L. (2006) Licensed to kill: the lifestyle of a necrotropic plant pathogen. *Trends Plant Sci.* **11,** 247–253
37. Zhou, N., Tootle, T. L., and Glazebrook, J. (1999) Arabidopsis PAD3, a gene required for camalexin biosynthesis, encodes a putative cytochrome P450 monooxygenase. *Plant Cell* **11,** 2419–2428
38. Schuhegger, H., Nafisi, M., Mansourova, M., Petersen, B. L., Olsen, C. E., Svatos, A., Halkier, B. A., and Glawischnig, E. (2006) CYP71B15 (PAD3)

catalyzes the final step in camalexin biosynthesis. *Plant Physiol.* **141,** 1248–1254
39. Chiang, K. P., Niessen, S., Saghatelian, A., and Cravatt, B. F. (2006) An enzyme that regulates ether lipid signaling pathways in cancer annotated by multidimensional profiling. *Chem. Biol.* **13,** 1041–1050
40. Madsen, M. A., Deryugina, E. I., Niessen, S., Cravatt, B. J., and Quigley, J. P. (2006) Activity-based protein profiling implicates urokinase activation as a key step ion human fibrosarcoma intravasation. *J. Biol. Chem.* **281,** 15997–16005
41. Schopfer, L. M., Voelker, T., Bartels, C. F., Thompson, C. M., and Lockridge, O. (2005) Reaction kinetics of biotinylated organiphosphorus toxicant, FP-biotin, with human acetylcholinesterase and human butyrylcholinesterase. *Chem. Res. Toxicol.* **18,** 747–754
42. Dijkstra, H. P., Sprong, H., Aerts, B. N., Kruithof, C. A., Egmond, M. R., and Klein Gebbink, R. J. (2008) Selective and diagnostic labelling of serine hydrolases with reactive phosphonate inhibitors. *Org. Biomol. Chem.* **6,** 523–531
43. Hamilton, J. M., Simpson, D. J., Hyman, S. C., Ndimba, B. K., and Slabas, A. R. (2003) Ara12 subtilisin-like protease from *Arabidopsis thaliana*: purification, substrate specificity and tissue localization. *Biochem. J.* **370,** 57–67
44. Rautengarten, C., Usadel, B., Neumetzler, L., Hartmann, J., Bussis, D., and Altmann, T. (2008) A subtilisin-like serine protease essential for mucilage release from Arabidopsis seed coats. *Plant J.* **54,** 466–480
45. Book, A. J., Yang, P., Scalf, M., Smith, L. M., and Vierstra, R. D. (2005) Tripeptidyl peptidase II. An oligomeric protease complex from Arabidopsis. *Plant Physiol.* **138,** 1046–1057
46. Yamauchi, Y., Eijri, Y., and Tanaka, K. (2003) Identification and biochemical characterization of plant acylamino acid-releasing enzyme. *J. Biochem.* **134,** 251–257
47. Shirley, A. M., and Chapple, C. (2003) Biochemical characterization of sinapoylglucose:choline sinapoyltransferase, a serine carboxypeptidase-like protein that functions as an acyltransferase in plant secondary metabolism. *J. Biol. Chem.* **278,** 19870–19877
48. Li, J., Lease, K. A., Tax, F. E., and Walker, J. C. (2001) BRS1, a serine carboxypeptidase, regulates BRI1 signaling in *Arabidopsis thaliana*. *Proc. Natl. Acad. Sci. U. S. A.* **98,** 5916–5921
49. Cummins, I., Landrum, M., Steel, P. G., and Edwards, R. (2007) Structure activity studies with xenobiotic substrates using carboxylesterases isolated from *Arabidopsis thaliana*. *Phytochemistry* **68,** 811–818
50. Kordic, S., Cummins, I., and Edwards, R. (2002) Cloning and characterization of an *S*-formylglutathione hydrolase from *Arabidopsis thaliana*. *Arch. Biochem. Biophys.* **399,** 232–238
51. Van Kan, J. A. L., Van't Klooster, J. W., Wagemakers, C. A. M., Dees, D. C. T., and Van der Vlught-Bergmans, C. J. B. (1997) Cutinase A of *Botrytis cinerea* is expressed, but not essential, during penetration of Gerbera and tomato. *Mol. Plant-Microbe Interact.* **10,** 30–38
52. Reis, H., Pfiffi, S., and Hahn, M. (2005) Molecular and functional characterization of a secreted lipase from *Botrytis cinerea*. *Mol. Plant Pathol.* **6,** 257–267